Magnetic Domain Structure and Magnetic Anisotropy in $Ga_{1-x}Mn_xAs$

U. Welp* and V. K. Vlasko-Vlasov
Materials Science Division, Argonne National Laboratory, 9700 South Cass Avenue, Argonne, Illinois 60439

X. Liu and J. K. Furdyna
Department of Physics, University of Notre Dame, Notre Dame, Indiana 46556

T. Wojtowicz
Department of Physics, University of Notre Dame, Notre Dame, Indiana and Institute of Physics, PAS, Warsaw, Poland
(Received 14 January 2003; published 24 April 2003)

Large, well-defined magnetic domains, on the scale of hundreds of micrometers, are observed in $Ga_{1-x}Mn_xAs$ epilayers using a high-resolution magneto-optical imaging technique. The orientations of the magnetic moments in the domains clearly show in-plane magnetic anisotropy, which changes through a second-order transition from a biaxial mode (easy axes nearly along [100] and [010]) at low temperatures to an unusual uniaxial mode (easy axis along [110]) as the temperature increases above about $T_c/2$. This transition is a result of the interplay between the natural cubic anisotropy of the GaMnAs zinc-blende structure and a uniaxial anisotropy which attribute to the effects of surface reconstruction.

DOI: 10.1103/PhysRevLett.90.167206 PACS numbers: 75.50.Pp, 75.30.Gw, 75.60.–d, 75.70.–i

Magnetic semiconductor alloys, such as epitaxial $Ga_{1-x}Mn_xAs$ films, have attracted considerable interest, since they hold unique potential for spintronics applications [1–4] in which information processing and storage is achieved by utilizing the spin degree of freedom of the electrons. In addition, the rich physical properties of $Ga_{1-x}Mn_xAs$ represent a remarkable manifestation of a strongly correlated system in which long-range magnetic order of the far spaced Mn ions is mediated by spin-polarized itinerant holes. As a consequence, one finds in this material properties not seen in conventional metallic ferromagnets, such as control of the magnetic state by light [5], electric fields [6], and strain. It has been shown that the magnetic anisotropy of $Ga_{1-x}Mn_xAs$ films is largely controlled by epitaxial strains [7], with tensile and compressive strains inducing in-plane and out-of-plane moment orientation, respectively. Theoretical models [8–10] based on hole-mediated magnetic order give a good account of the observed moment orientations, and the formation of magnetic domains is expected [9]. For the out-of-pane magnetized films stripe domain patterns were reported earlierd [11]. However, the magnetic structure of in-plane magnetized films—which are expected to form the basis for most applications, such as spin injectors [12], tunnel junctions [13], or giant planar Hall effect devices [14]—remains largely unknown.

Here we present a study of in-plane magnetized $Ga_{1-x}Mn_xAs$ samples that combines direct imaging of magnetic domains and SQUID magnetometry. We observe clear evidence for an unusual temperature-dependent in-plane magnetic anisotropy. At temperatures above about $T_c/2$ the samples show uniaxial anisotropy with an easy axis along the [110] direction, whereas at temperatures below $T_c/2$ two easy axes emerge in a second-order transition which approach the [100] and [010] directions as the temperature decreases. This transition is a result of the competition between the cubic anisotropy of $Ga_{1-x}Mn_xAs$ and the uniaxial *growth induced* anistropy in the film plane. The former is dominated by the strong, temperature-dependent coupling between spin-polarized itinerant holes and localized Mn moments [10], whereas the latter can arise from surface reconstruction [15]. Here, we present the first direct images of magnetic domains showing that even though the Mn moments are diluted, the magnetization reversal proceeds through the nucleation and expansion of large (several hundred microns), well-defined domains. In the biaxial state we observe 90° domains, and in the uniaxial state 180° domains are observed. The domain boundaries show some roughness and pinning that is indicative of some degree of sample inhomogeneity.

The $Ga_{1-x}Mn_xAs$ samples were grown on (001) GaAs substrates using molecular beam epitaxy, as described in detail previously [16]. The results presented here were obtained on an unannealed 300 nm thick sample with $x \approx 0.03$ (as determined from the lattice constants) and $T_c \approx 60$ K. Similar results were also observed on a sample with a slightly higher value of x. The magnetic characterization was performed in a SQUID magnetometer. The magnetic domains were imaged using a magneto-optical technique that utilizes a Bi-doped garnet layer as an optical magnetic field sensor [17]. The in-plane magnetized garnet layer, with a mirror on one side, is placed directly on the sample, with the mirror side adjacent to the sample. Magnetic stray fields emanating from the sample induce Faraday rotation in the garnet, which is visualized in a polarized light microscope. We note that this imaging technique does not perturb the

magnetic state of the sample. Since the light is confined to the garnet layer, photo-induced magnetization changes that could arise in conventional Kerr microscopy are avoided. In addition, remagnetization of the sample such as seen during magnetic-force microscopy on magnetically soft samples [18] does not occur.

Figures 1(a) and 1(b) show magnetization curves at 15 and 35 K for fields along the in-plane $[\bar{1}10]$, [110], and [100] directions. A distinct in-plane anisotropy of the magnetization is clearly revealed. At 15 K, [100] is the easy axis, with essentially the full moment at remanence. Nevertheless, magnetization reversal starts gradually close to $H = 0$ [see inset of Fig. 1(a)], followed by sharp switching at the coercive field of 28 Oe. Hard-axis-like behavior is seen for the $[\bar{1}10]$ direction with saturation occurring around 1.5 kOe. The magnetization curves for the [100] and [010] directions are identical. The difference in behavior for the $[\bar{1}10]$ and [110] directions is not expected on the grounds of crystal symmetry, and will be discussed in detail below. At 35 K the easy axis has switched to the [110] direction, whereas the $[\bar{1}10]$ direction displays typical hard-axis behavior, with essentially zero remanence. The temperature dependence of the saturation magnetization, M_s, is shown in the inset of Fig. 1(b). The size of M_s and its upward curvature near T_c are typical for samples of similar composition [19].

Figure 2 (top) shows domain images at 15 K taken near a corner of the sample for fields applied along the easy [100] direction indicated in frame 2(a). In the positively polarized remanent state (Fig. 2(a)) magnetic contrast arises only at the sample edges seen as white lines and near a defect at the left edge. With the application of a reversal field [Fig. 2(b)] a transversely polarized domain nucleates at the corner of the sample. The moment orientation of this domain is revealed by the contrast at the edges (a more detailed discussion of the orientations will be given below). While the contrast at the right edge remains unchanged, the contrast on the left turns dark, indicating the reversal. The domain boundary appears as a jagged bright line consistent with the indicated moment orientations. The transverse domain expands with increasing field [Fig. 2(c)]. Then a totally reversed domain nucleates at the left edge [Fig. 2(d)], and spreads rapidly through the entire sample [Fig. 2(e)]. The magnetization reversal through an intermediate (nearly) 90° domain state is typical for samples displaying biaxial magnetic anisotropy. It accounts for the two stages in the magnetization hysteresis for the easy axes seen in Fig. 1(a).

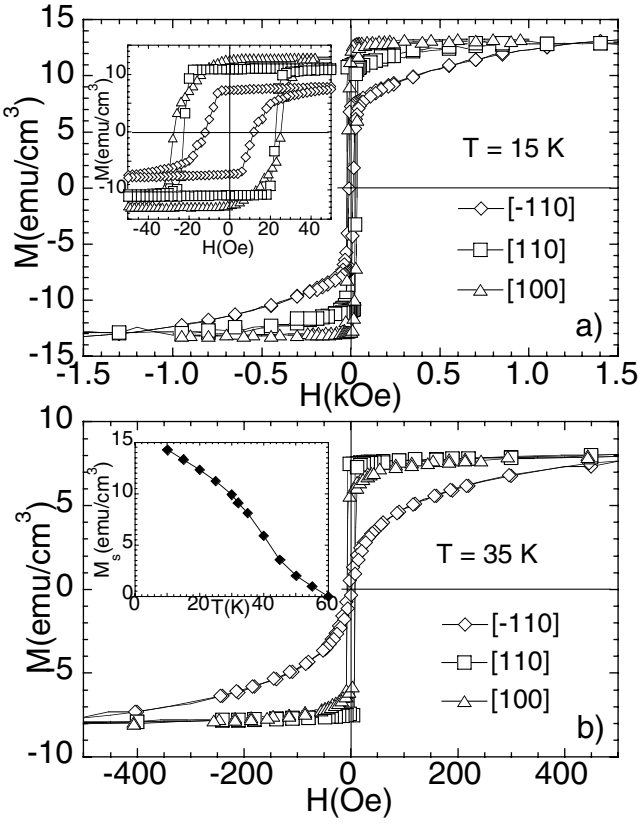

FIG. 1. Magnetization curves at 15 K (a) and 35 K (b) along different crystallographic directions. Inset (a): expanded presentation of the data at 15 K; inset (b): temperature dependence of the saturation magnetization, M_s.

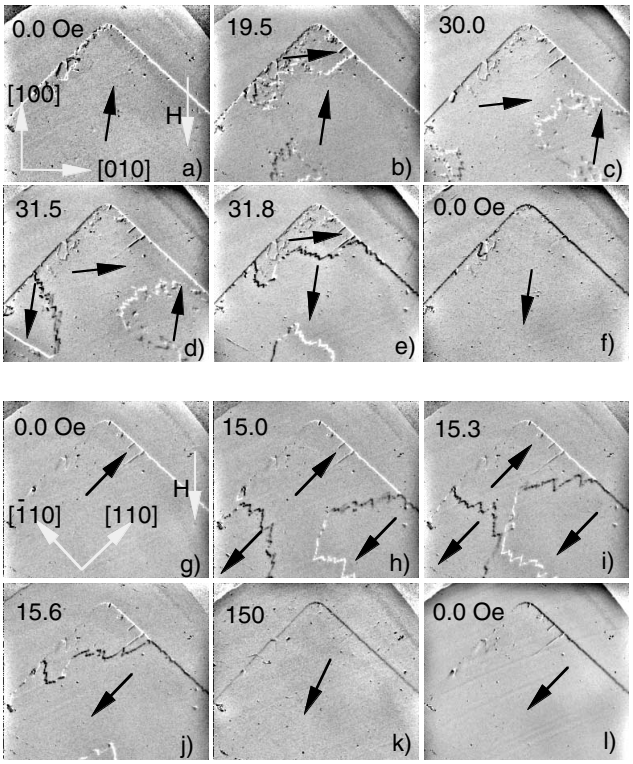

FIG. 2. Magneto-optical domain images taken near a corner of the sample at 15 K [top panels: (a) to (f)] and at 35 K [bottom panels: (g) to (l)] in the indicated fields applied along the [100] direction (vertical axis). The frame width is 1 mm. Positive (negative) perpendicular fields are seen as bright (dark) contrast. Black arrows indicate the orientation of the magnetic moments in the domains.

Figure 2 (bottom) shows domain images at 35 K. In the remanent states [Figs. 2(g) and 2(l)] magnetic contrast appears only at the right edge, indicating a moment orientation along [110]. During magnetization reversal 180° domains nucleate and expand [Figs. 2(h)–2(j)], as is typical for magnetic systems with uniaxial anisotropy. The zig-zag domain boundaries are clearly visible. Contrast at the left edge of the sample appears only in elevated fields [Fig. 2(k)] when the magnetization is pulled into the field direction. Figure 2 thus demonstrates that on increasing the temperature the magnetic anisotropy changes from biaxial, with easy axes approximately along [100] and [010], to uniaxial, with easy axis along [110].

The magnetization reversal at 35 K along the easy axis proceeds through the nucleation and expansion of 180° domains shown in Fig. 3. Specifically, we notice a pronounced domain wall creep: images 3(b)–3(d) are taken in the same applied field at time intervals of about 30 sec. In this regime the shape of the domain boundary appears to be determined by isolated strong pinning centers inducing the scalloped boundary.

The evolution of the above magnetization behavior can be described in a model that includes a biaxial, a uniaxial, and a Zeeman term in the energy: $E = K_{1c}\sin^2(\phi)\cos^2(\phi) + K_{1u}\sin^2(\phi) - M_s H\cos(\phi - \phi_0)$. Here K_{1c} and K_{1u} are the first order cubic and uniaxial anisotropy constants, and the angles ϕ and ϕ_0 measure the moment orientation and field orientation with respect to the uniaxial [110] axis [see inset of Fig. 4(a)]. Then, $K_{1c} < 0$ yields easy axes along [100] and [010] in the absence of the uniaxial contribution. In the presence of the uniaxial term the system is uniaxial with [110] as easy axis for $K_{1u} > -K_{1c}$, whereas for $K_{1u} < -K_{1c}$ it is biaxial with easy axes at angles given by $\cos(2\phi) = -K_{1u}/K_{1c}$.

The orientation of the easy axes can be conveniently determined by imaging the magnetic contrast at remanence around a hole patterned into the sample [17]. The inset of Fig. 4(b) shows magneto-optical images around an 80-μm hole at 16 and 34 K. The rotation of the contrast, i.e., the moment direction, is clearly seen. Following these images as a function of temperature yields the temperature dependence of the easy-axis orientation, as shown in Fig. 4(b). Alternatively, the moment orientation can be obtained by determining K_{1c} and K_{1u} from fits of the hard-axis magnetization curves ($\phi_0 = \pi/2$) and calculating the easy-axis orientation form the above relation. The hard-axis magnetization curve is given by $H = [2(K_{1u} + K_{1c})/M_s]\sin(\phi) - [4K_{1c}/M_s]\sin^3(\phi)$. The results for the anisotropy fields $2K_{1u}/M_s$ and $2K_{1c}/M_s$ are shown in Fig. 4(a), and the easy-axis orientation is shown in Fig. 4(b). The calculated moment orientation agrees well with the magneto-optical determinations, indicating good consistency of the data. As the temperature decreases below 32 K, the moment orientation starts to deviate from the [110] direction in a continuous fashion, indicating a second-order magnetic transition, with the angle ϕ being the order parameter.

The values for the anisotropy fields [Fig. 4(a)] are in good overall agreement with results obtained from FMR experiments [16]. Near T_c the uniaxial term is dominant. While this term increases slowly with decreasing temperature, the biaxial term increases (in magnitude) rapidly below 30 K, triggering the transition from uniaxial to biaxial anisotropy. A temperature-induced change in magnetic anisotropy has very recently also been reported in $Ga_{1-x}Mn_xAs$ with low hole concentration, $T_c \approx 24$ K

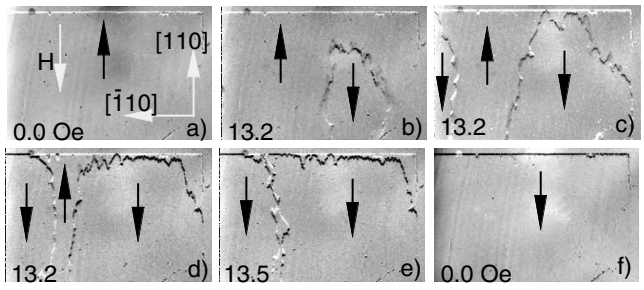

FIG. 3. Magneto-optical images at 35 K in fields applied along the [110] direction. The width of the frames is 1 mm.

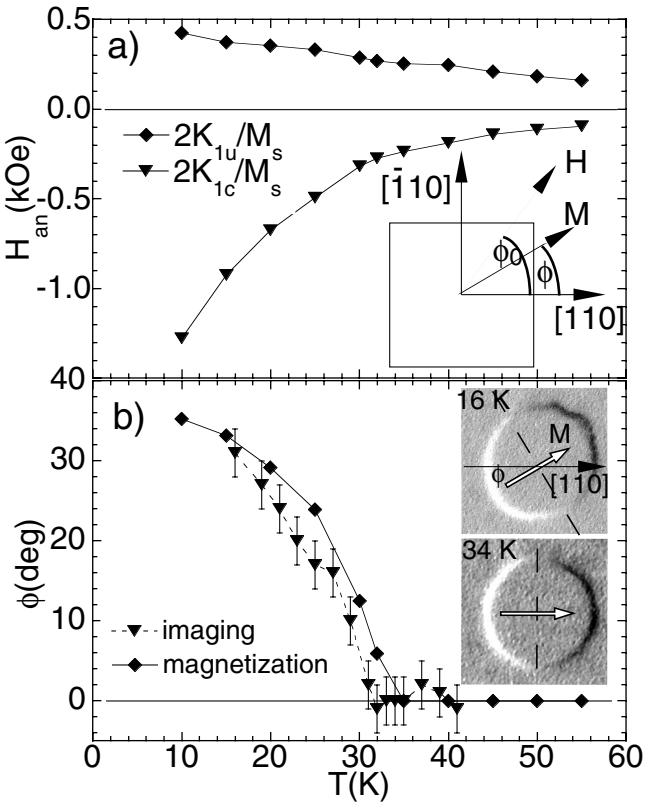

FIG. 4. (a) Temperature dependence of the in-plane uniaxial and cubic anisotropy fields. The inset defines the experimental geometry. (b) Temperature dependence of the angle of the easy axis with respect to the [110] direction. The inset shows the magneto-optical contrast around an 80-μm hole at 16 and 34 K, which identifies the moment orientation at $H = 0$.

[20]. Generally, a strong temperature dependence of the anisotropy at low temperatures is unusual in conventional ferromagnets. In $Ga_{1-x}Mn_xAs$ it has been ascribed to the intimate coupling of the local magnetic moments on the Mn sites and itinerant holes that mediate long-range magnetic order. It has been suggested [20,21] that with decreasing temperature holes become localized at the Mn site causing an increase of the anisotropy due to enhanced spin-orbit coupling. The increase of the resistivity at low temperatures seen frequently in samples of similar composition has been interpreted as an indication of such hole localization.

The presence of a small uniaxial anisotropy in the film plane has been noted before [14,16,20,22]. Our results show that this term in fact has a profound influence on the magnetic structure of $Ga_{1-x}Mn_xAs$. The occurrence of this term is not expected on the basis of the cubic zinc-blende structure of bulk $Ga_{1-x}Mn_xAs$. However, it has been shown that epitaxial bcc Fe-films deposited on (001) GaAs substrates also display uniaxial anisotropy along a [110] direction [15]. It is believed that this anisotropy is a consequence of the arrangement of bonds at the GaAs-surface and subsequent surface reconstruction. As-dimerization can induce 2×4 and $c(4 \times 4)$ reconstructed surfaces in which the $[\bar{1}10]$ and [110] directions are *inequivalent*, thus causing a uniaxial anisotropy. Surface reconstruction has been observed during the growth of $Ga_{1-x}Mn_xAs$/GaAs [7], and it is expected that a uniaxial anisotropy can be seeded at the $Ga_{1-x}Mn_xAs$/GaAs interface similar to that observed in the Fe/GaAs-samples. An additional contribution to the anisotropy can also arise from anisotropic relaxation of strains induced by the lattice mismatch [23]. X-ray analysis indicates that $Ga_{1-x}Mn_xAs$ films of up to a thickness of 2 μm remain tetragonally strained [24]. However, due to the strong strain effects, even small anisotropic strain relaxation can generate anisotropies of the size observed here.

$Ga_{1-x}Mn_xAs$ is generally considered a random alloy with a low concentration of magnetic ions. Recent results [25] indicate that clustering and rearrangement of mobile Mn-interstitials are crucial for determining the electronic structure. Notwithstanding, we do not observe any incoherent magnetization reversal on small length scales. Instead, Figs. 2–4 show that the magnetization reversal in our $Ga_{1-x}Mn_xAs$ samples proceeds through the nucleation and rapid expansion of large, well-defined domains and that the magnetization reversal of $Ga_{1-x}Mn_xAs$ is similar to that of conventional ferromagnets. These findings are in contrast to an earlier report on inhomogeneous magnetic structures in in-plane magnetized $Ga_{1-x}Mn_xAs$ [26].

In summary, we observe clear evidence for a temperature dependent in-plane magnetic anisotropy in $Ga_{1-x}Mn_xAs$. Above about $T_c/2$ the samples show uniaxial anisotropy with easy axis along a [110] direction, whereas below $T_c/2$ two easy axes emerge in a second-order transition, which at low temperatures approach the [100] and [010] directions. Even though the Mn moments are diluted and located randomly, the magnetization reversal proceeds through the nucleation and expansion of large (several hundred microns), well-defined domains. In the biaxial state 90° domains and in the uniaxial state 180° domains are observed.

This work was supported by the U.S. Department of Energy, BES under Contract No. W-31-109-ENG-38, by the DARPA SpinS Program, and by the NSF under Grant No. DMR02-10519.

*Electronic address: welp@anl.gov

[1] H. Ohno *et al.*, Science **281**, 951 (1998).
[2] G. A. Prinz, Science **282**, 1660 (1998).
[3] J. K. Furdyna *et al.*, in *Optical Properties of Semiconductor Nanostructures*, NATO Science Series Vol. 81, edited by M. L. Sadowski, M. Potemski, and M. Grynberg (Kluwer, Dordrecht, 2000), p. 211.
[4] S. A. Wolf, Science **294**, 1660 (2001).
[5] S. Koshihara *et al.*, Phys. Rev. Lett. **78**, 4617 (1997); A. Oiwa *et al.*, Phys. Rev. Lett. **88**, 137202 (2002).
[6] H. Ohno *et al.*, Nature (London) **408**, 944 (2000).
[7] A. Shen *et al.*, J. Cryst. Growth **175/176**, 1069 (1997).
[8] J. König, T. Jungwirth, and A. H. McDonald, Phys. Rev. B **64**, 184423 (2001).
[9] T. Dietl, J. König, and A. H. McDonald, Phys. Rev. B **64**, 241201 (2001).
[10] T. Dietl, H. Ohno, and F. Matsukura, Phys. Rev. B **63**, 195205 (2001).
[11] T. Shono *et al.*, Appl. Phys. Lett. **77**, 1363 (2000).
[12] G. Schmidt *et al.*, Phys. Rev. Lett. **87**, 227203 (2001).
[13] D. Chiba *et al.*, Appl. Phys. Lett. **77**, 1873 (2000); M. Tanaka and Y. Higo, Phys. Rev. Lett. **87**, 026602 (2001).
[14] H. X. Tang *et al.*, cond-mat/0210118.
[15] J. J. Krebs, B. T. Jonkers, and G. A. Prinz, J. Appl. Phys. **61**, 2596 (1987); M. Kneedler *et al.*, Phys. Rev. B **56**, 8163 (1997).
[16] X. Liu, Y. Sasaki, and J. Furdyna, Phys. Rev. B (to be published).
[17] V. Vlasko-Vlasov *et al.*, Phys. Rev. Lett. **86**, 4386 (2001); L. A. Dorosinski *et al.*, Physica (Amsterdam) **203C**, 149 (1992).
[18] U. Welp *et al.*, Appl. Phys. Lett. **79**, 1315 (2000).
[19] J. K. Furdyna *et al.*, J. Appl. Phys. **91**, 7490 (2002).
[20] M. Sawicki *et al.*, cond-mat/0212511.
[21] M. Rubinstein *et al.*, J. Magn. Magn. Mater. **250**, 164 (2002).
[22] D. Hrabovski *et al.*, Appl. Phys. Lett. **81**, 2806 (2002).
[23] Y. B. Xu *et al.*, Phys. Rev. B **62**, 1167 (2000).
[24] A. Shen *et al.*, J. Cryst. Growth **201/202**, 679 (1999).
[25] K. M. Yu *et al.*, Phys. Rev. B **65**, 201303 (2002); M. van Schilfgaarde and O. N. Mryasov, *ibid.* **63**, 233205 (2002).
[26] T. Fukumura *et al.*, Physica (Amsterdam) **10E**, 135 (2001).